

The Phase Diagram of the Flory–Huggins–de Gennes Model of a Binary Polymer Blend

Bruce M. Forrest^{1,2} and Raúl Toral¹

Received November 23, 1993; final March 22, 1994

We undertake a numerical study of the Flory–Huggins–de Gennes functional in $d=3$ dimensions describing a polymer blend. By discretising the functional on a three-dimensional lattice and employing the hybrid Monte Carlo simulation algorithm, we investigate to what extent the inclusion of the term describing fluctuations in local polymer concentration alters the phase diagram of the model. We find that, despite the relatively small weight of the fluctuation term, the coexistence curve is shifted by an appreciable amount from that predicted by naive mean-field theory, which ignores such spatial fluctuations. The direction of the shift is consistent with that already observed in experiment and in simulations of microscopic models of polymer blends. A finite-size scaling analysis indicates that the critical behavior of the model seems to belong to the 3D Ising universality class rather than being mean-field in nature.

KEY WORDS: Polymer blend; Flory–Huggins–de Gennes free energy; hybrid Monte Carlo; finite-size scaling.

1. INTRODUCTION

The Flory–Huggins (FH) model^(1–3) has become a well-established basis for the thermodynamic description of A – B polymer mixtures. Its original formulation consists in placing the monomers and solvent molecules on a lattice and so has the advantage that the excluded-volume criterion, which is otherwise intractable analytically, is automatically accounted for by demanding that each lattice site be occupied exclusively by a monomer or

It is a pleasure to dedicate this paper to Oliver Penrose on the occasion of his 65th birthday.

¹ Departament de Física, Universitat de les Illes Balears, E-07071 Palma de Mallorca, Spain.

² Present address: Institut für Polymere, ETH Zürich, CH-8092 Zürich, Switzerland.

a solvent molecule. It is also well suited to allow for the large number of configurations available to each polymer.

However, FH "theory" itself does not constitute a full solution of this lattice model, but is rather a mean-field approximation which incorporates a number of simplifications⁽⁴⁾ over an above the assumption of an underlying lattice structure. Within this mean-field approximation the free energy of mixing per lattice site in FH theory is, in the absence of vacancies, given by⁽¹⁾

$$f_{\text{FH}}(\phi) \equiv \frac{F}{k_{\text{B}}T} = \frac{\phi}{N_A} \ln \phi + \frac{1-\phi}{N_B} \ln(1-\phi) + \chi\phi(1-\phi) \quad (1)$$

where ϕ (resp., $1-\phi$) is the local concentration of polymers of type A (resp., B), each consisting of N_A (resp., N_B) monomers; and where χ is the so-called Flory-Huggins interaction parameter. In this formulation χ is independent of ϕ and of the length of the polymers; it is purely a function of temperature, $\chi \propto 1/T$.

This, however, has proved to be one of the major deficiencies of the FH theory; experimental evidence has shown that, taking (1) at face value and interpreting χ as a phenomenological parameter, one is left with an effective χ ,⁽⁵⁾ which is a function of ϕ and, possibly, of N . Numerical simulations of the lattice model^(4,6) from which the FH theory stems have also been at variance with the predictions of (1), showing that the failings of the theory must arise, at least in part, from the inherent mean-field assumptions used in obtaining (1) and are not necessarily due to the underlying lattice model. Such discrepancies between the classical FH mean-field theory and experimental and numerical findings have led to the inclusion of refinements and extensions of the original theory.⁽⁷⁻⁹⁾

One such extension, which we shall be concerned with in this study, involves a coarse-grained description of the polymer mixture in terms of the mean concentration ϕ . All fluctuations on small length scales, including the internal degrees of freedom of the polymers, are averaged out and only the slower, long-wavelength, spatial variations of ϕ are included. This field-theoretic approach can be regarded as a type of Ginzburg-Landau formulation of the original problem. Specifically, the system is described by the Flory-Huggins-de Gennes (FHdG) free-energy functional⁽¹⁰⁻¹²⁾

$$\frac{\mathcal{F}[\phi]}{k_{\text{B}}T} = \int d\mathbf{x} \left\{ f_{\text{FH}}(\phi(\mathbf{x})) + \frac{a^2}{36\phi(\mathbf{x})[1-\phi(\mathbf{x})]} (\nabla\phi)^2 \right\} \quad (2)$$

where the characteristic length a is given by $a^2/[\phi(1-\phi)] = l_A^2/\phi + l_B^2/(1-\phi)$, with each A (B) polymer having subunits of length l_A (l_B). (In the particular case of $l_A = l_B$, one has $a = l$.) The polymer aspect

is contained in the FH free-energy expression f_{FH} [Eq. (1)], while the gradient term accounts for the free-energy contribution of spatial variations in the local concentration field ϕ . This, however, is only the first term of an expansion which assumes that such spatial variations are slow,^(12,13) so (2) is only valid when the gradient term is small in comparison to the single-site contribution of $f_{\text{FH}}(\phi)$.

The FH mean-field theory is obtained from (2) by ignoring any such spatial fluctuations: $\phi(\mathbf{x}) = \phi_{\text{MF}}, \forall \mathbf{x}$, where ϕ_{MF} is that value of ϕ which minimizes $f_{\text{FH}}(\phi)$. We henceforth refer to this as the “bare” mean-field theory of the model; any spatial fluctuations in the local concentration field ϕ are neglected. An appealing aspect of this bare mean-field theory is that analytical expressions for thermodynamic quantities of interest are readily obtainable. In particular, one can obtain a closed expression for the coexistence curve on the phase diagram which separates the homogeneous one-phase region (where the two constituent types of polymers freely mix) from the two-phase regime (where the two types segregate, forming macroscopic regions rich in each type of polymer). In fact the FHdG free energy was introduced in order to study the dynamics of phase separation following a quench into the unstable part of the phase diagram where the system evolves by spinodal decomposition. In this context, the FHdG free energy has been used in numerical studies of the Cahn–Hilliard–Cook evolution equations.^(14–16) The dynamics of phase separation has also received recent attention in the context of lattice models.^(17–19)

Despite the availability of the full FHdG functional (2), most experimental and computational investigations adopt the simpler bare mean-field theory (1) as a reference point. However, given the aforementioned shortcomings of this theory, it seems appropriate to determine to what extent the predictions of the full field-theoretic description (2) differ from (and improve upon) the mean-field theory. For example, even though the spatial term in (2) may be small, what effect does its neglect have on the phase diagram of the model? The location of the phase diagram is of fundamental importance in studying phase-separation phenomena in polymer mixtures, since the subsequent time evolution is determined by the position of the quench inside the coexistence curve. Although a Ginzburg-like criterion⁽²⁰⁾ would imply that the FH theory is exact in the large- N limit, previous numerical studies of the FH lattice model⁽⁶⁾ and a related bond-fluctuation model^(21–23) reveal large discrepancies with respect to the bare mean-field theory in the location of the critical point and the coexistence curve.

In this contribution we want to determine the suitability of the FH theory to describe the equilibrium properties of a system defined by the FHdG free energy. We address this question by undertaking a numerical

study of (2) and comparing our estimates of thermodynamic variables with those predicted by the classical, bare FH theory. In particular, we determine the phase diagram in terms of the FH interaction parameter χ and the polymer length N . We find that, as expected, the behavior of the system in the critical region is better described by the Ising critical exponents than by the mean-field ones. More interestingly, and in the same vein as the lattice-simulation results, our study shows important discrepancies far from criticality in the values of thermodynamic quantities, namely the order parameter and the susceptibility. Our study also demonstrates the convenience of the hybrid Monte Carlo method in sampling a complicated free energy functional.

2. METHOD

We restrict ourselves to the symmetric case in which the two constituent types of polymer are of identical sizes: $N_A = N_B = N$ and $l_A = l_B = 1$ ($\rightarrow a = 1$). The functional integration (2) is performed numerically on a three-dimensional lattice of L^3 vertices and mesh size Δx . In effect, we use the following discretized free energy:

$$\frac{F[\phi]}{k_B T} = \sum_{\mathbf{x}} (\Delta x)^3 \left[f_{\text{FH}}(\phi_{\mathbf{x}}) + \frac{1}{36\phi_{\mathbf{x}}(1-\phi_{\mathbf{x}})} \frac{1}{2} \sum_{\mathbf{y}} \left(\frac{\phi_{\mathbf{y}} - \phi_{\mathbf{x}}}{\Delta x} \right)^2 \right] \quad (3)$$

where the $2d = 6$ nearest neighbors of \mathbf{x} are denoted by \mathbf{y} . The thermodynamics of the system is given by the partition function $\mathcal{Z} = \int [d\phi] \exp(-F[\phi]/k_B T)$. In this symmetric case one has, from (1),

$$f_{\text{FH}}(\phi) = \frac{1}{N} [\phi \ln \phi + (1 - \phi) \ln(1 - \phi)] + \chi \phi(1 - \phi)$$

Hence, (3) is symmetric under $\phi_{\mathbf{x}} \leftrightarrow 1 - \phi_{\mathbf{x}}$. The function $f_{\text{FH}}(\phi)$ has a double-well structure, signaling the possibility of coexistence of the two phases, as in the case of the ϕ^4 model. However, in contrast to the ϕ^4 model, in which the field can assume any real value, in the present case the concentration fields $\phi_{\mathbf{x}}$ are restricted to the interval $0 \leq \phi_{\mathbf{x}} \leq 1$.

In order to sample the Boltzmann probability distribution $P_B([\phi]) = \mathcal{Z}^{-1} \exp(-F[\phi]/k_B T)$, we employed the hybrid Monte Carlo (HMC) method. Originally proposed in the context of lattice gauge theories,⁽²⁴⁾ this global-update algorithm has now become a well-recognized simulational tool in condensed-matter problems.⁽²⁵⁾ A general advantage of the HMC method which is particularly useful in this problem is that it provides direct

access to the Boltzmann distribution and avoids the need to split up the functional (3) or to employ any approximative steps.

Our strategy for obtaining the coexistence curve in terms of χ and N was as follows. For fixed values of χ we located the critical polymer length N_c separating the homogeneous one-phase region from the two-phase region. We then determined the coexistence curve (the mean concentration) at values of $N > N_c$, i.e., in the two-phase region. In bare FH mean-field theory the critical polymer length is simply given by $N_c^{\text{MF}} = 2/\chi$ and the coexistence curve is obtained by minimizing (1) with respect to ϕ :

$$\frac{1}{N} \ln \left(\frac{\phi_{\text{coex}}^{\text{MF}}}{1 - \phi_{\text{coex}}^{\text{MF}}} \right) = \chi (2\phi_{\text{coex}}^{\text{MF}} - 1) \quad (4)$$

Since (3) is invariant under $\phi_x \leftrightarrow 1 - \phi_x$, and hence is symmetric about $\phi_x = \frac{1}{2}$, we define an order parameter $M \equiv L^{-3} \sum_{\mathbf{x}} (2\phi_{\mathbf{x}} - 1) \in [-1, 1]$. Here M is analogous to the “magnetization” per site in the discrete ϕ^4 model and its distribution is symmetric about zero. In the one-phase region we have $\langle M \rangle = 0$ (where $\langle \dots \rangle$ denotes a canonical average), while the two-phase region has $\langle M \rangle = \pm M_{\text{coex}} \neq 0$. However, since for finite systems the free-energy barrier between these two minima in the free-energy distribution can never be infinite, the correct observable to measure for odd moments of M in a simulation is $\langle |M| \rangle$.⁽²⁶⁾

We have adopted a reparametrization in (3), in a similar vein to ref. 16, where $\mathbf{x}^* \equiv (\chi - 2/N)^{1/2} \mathbf{x}$ with $\Delta \mathbf{x}^* = 1$ is advocated. This has the effect of producing a larger Δx in the original parametrization (3) and thus helps ensure that the weight of the discretized gradient term is small compared to the contribution of $f_{\text{FH}}(\phi_x)$. However, in the present study we wish to maintain a *constant* mesh size Δx for all values of χ and N ; such a χ - and N -dependent scale factor would complicate finite-size scaling analyses. We hence chose a fixed scale factor: one that would correspond to $\chi = 0.004$, $N = 600$ in ref. 16, i.e., $\mathbf{x}^* \approx \mathbf{x}/40$. We found that with this parametrization the weight of the interaction term in (3) was mostly of the order of a few percent for the range of χ and N which we considered.

3. COMPARISON WITH MEAN-FIELD THEORY

In Fig. 1 we show, for fixed $\chi = 0.004$, the average order parameter $\langle |M| \rangle$ as a function of polymer length N for three different system sizes: $L^3 = 4^3$, 8^3 , and 16^3 lattice sites. It can be seen that the location of the coexistence curve is, of course, also system-size-dependent in addition to being a function of χ and N , i.e., we have $M_{\text{coex}} = M_{\text{coex}}(\chi; N, L)$. For increasing L , the curve approaches the N axis more steeply and in the

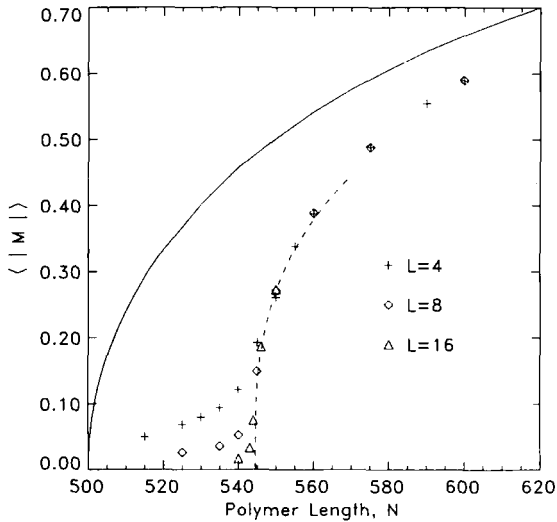


Fig. 1. The average order parameter $\langle |M| \rangle$ as a function of polymer length N with a fixed value $\chi = 0.004$ of the Flory interaction parameter for different system sizes L^3 . The solid line is the prediction of the mean-field theory. The dashed line is a fit to the behavior $\langle |M| \rangle \sim |1 - N/N_c|^\beta$ with $N_c = 544$ and $\beta = 0.324$.

thermodynamic limit, $M_{\text{coex}}(\chi; N, \infty)$, it would approach it vertically, vanishing at the critical polymer length N_c . For $N < N_c$ we are in the homogeneous one-phase region, with $\langle |M| \rangle = 0$, while above N_c , in the two-phase region, we would have $\langle |M| \rangle = M_{\text{coex}}(\chi; N, \infty) \neq 0$. An estimate for the behavior of $M_{\text{coex}}(\chi; N, \infty) \sim |1 - N/N_c|^\beta$ is also given in the figure, as will be explained below. The L dependence of the curve becomes weaker as N increases away from N_c into the two-phase region. At these larger values of N , simulations with smaller system sizes therefore suffice in order to locate the coexistence curve accurately.

The mean-field estimate for M_{coex} vanishes at $N_c^{\text{MF}} = 2/\chi = 500$. It is, however, obvious from the figure that both the values of the critical point and the location of the coexistence curve itself are overestimated by the theory. Note that, from the tendency of the curve to shift down and to the right as L increases (i.e., away from the mean-field curve), we can conclude that the curve for any given (finite) value of L provides a lower bound on the deviation from the mean-field theory.

In order to obtain an estimate for the critical polymer length N_c given by (3), we first plotted the susceptibility $\chi_s \equiv L^d(\langle M^2 \rangle - \langle |M| \rangle^2)$ as a function of N in Fig. 2. This should diverge with increasing L as $N \rightarrow N_c$.

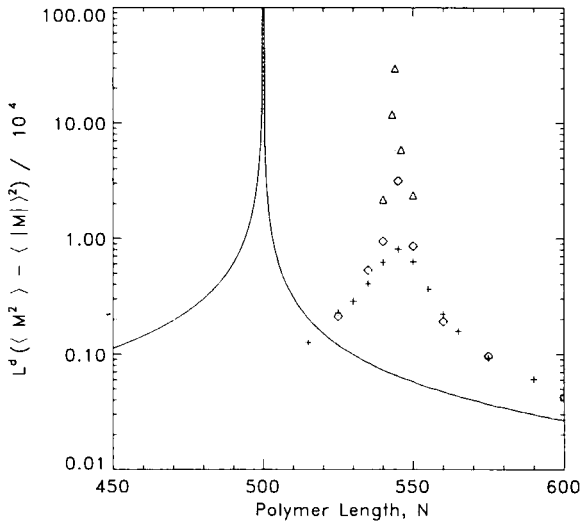


Fig. 2. Susceptibility in the same case as in Fig. 1. The solid line is the prediction of bare mean-field theory. Same symbols as Fig. 1.

Also shown in the figure is the estimate given by the mean-field theory, which is

$$\chi_s^{\text{MF}} = \frac{N}{1/\phi(1-\phi) - 2N\chi} \tag{5}$$

with $\phi = \phi_{\text{coex}}^{\text{MF}}$ from (4). This can be derived by adding an external field H in (1) to obtain $f_{\text{FH}}(\phi) - \beta H\phi$, where $\beta = 1/k_B T$. The mean-field solution is then given by $f'_{\text{FH}}(\phi^{\text{MF}}) = \beta H$, whence

$$\chi_s^{\text{MF}} \equiv [\partial\phi^{\text{MF}}/\partial(\beta H)]_{H=0} = 1/f''_{\text{FH}}(\phi_{\text{coex}}^{\text{MF}})$$

An estimate for N_c is more readily obtained from the behavior of the ratio $\langle M^2 \rangle / \langle |M| \rangle^2$. In the one-phase region this quantity approaches the limiting value $\pi/2$ as $L \rightarrow \infty$, whereas it approaches unity in the two-phase region.⁽²⁷⁾ The rate at which it changes from one limiting value to the other increases with L as the critical region is traversed. Curves for different L (assuming L is large enough) should intersect each other at the critical point.⁽²⁷⁾ From Fig. 3 we can conclude that $542 < N_c < 545$. This is in good agreement with the estimates for the critical value which could be extracted from Figs. 1 and 2.

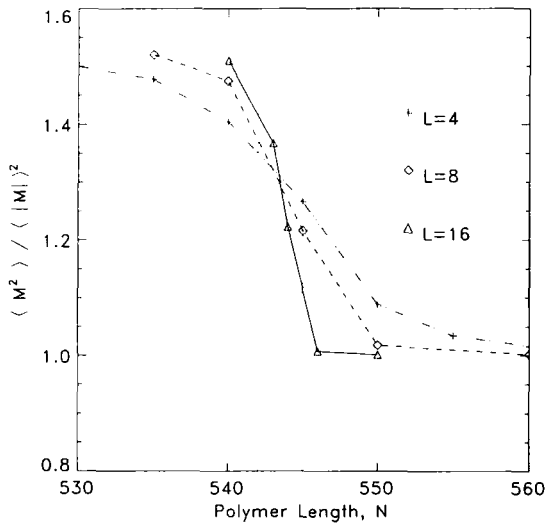


Fig. 3. The order parameter cumulant in the same case as in Fig. 1. The vertical dotted lines denote the bounds on the location of the critical point defined as the value of the polymer length N for which the cumulant is independent of system length L .

Using these bounds on N_c , we now investigate the finite-size scaling behavior of the model. Due to the increase in the range of the effective interactions with increasing length N in a real polymer mixture, it is expected from the Ginzburg criterion^(20,28) that the region around the critical point in which Ising-like scaling behavior is displayed should shrink as N becomes larger. Outside of this region the mean-field approximation should hold and hence finite-size scaling behavior with mean-field exponents should be exhibited. Within the framework of the discretized model (3), with χ fixed and $1/N$ an adjustable parameter (controlling the relative weight of the single-site coefficient), since the interaction term has a constant (N -independent) coefficient, we would expect such finite-size scaling behavior to be

$$\langle |M| \rangle = L^{-v} f(L^u(1 - N/N_c)) \quad (6)$$

[Note that, unlike in a microscopic polymer model, the number of degrees of freedom in (3) is always L^d , independent of N .] For Ising-like scaling behavior we would have, due to hyperscaling, $u = 1/\nu$ and $v = \beta/\nu$,⁽²⁷⁾ with, in $d = 3$ dimensions, $\beta = 0.324$ and $\nu = 0.629$,⁽²⁹⁾ whereas the corresponding mean-field exponents would be $u = d/2 = 3/2$ and $v = d/4 = 3/4$.⁽²⁷⁾ Given the estimated location of N_c from Fig. 1, we have tested the validity of both

forms of scaling in Fig. 2. Data for $L = 12$ are also included. They were left out of Fig. 1 in the interests of clarity. Figure 4 shows the best data collapse obtained with the Ising exponents, which occurs at $N_c = 544$. The corresponding data collapse with the mean-field exponents is displayed in Fig. 5 and occurs at $N_c = 542$. It is obvious that the behavior is much better described by Ising-like finite-size scaling in this instance. The $L \rightarrow \infty$ limit of (6), given by $\langle |M| \rangle \propto |1 - N/N_c|^{v/u}$, is also indicated both in Fig. 2 and in Fig. 1, where the Ising case gives $v/u = \beta$.

In order to ascertain whether the observed discrepancy of the model (3) with the predicted mean-field behavior (both with respect to the location of the coexistence curve and the finite-size scaling) holds in general and is not just an artefact of choosing, e.g., “small” values of N , we repeated the above analysis for other, smaller values of χ . Figure 6 is essentially of the same form as Fig. 1, except that the N dependence on the horizontal axis is displayed as $2/N\chi$. We have included data at two other values of χ ($=0.001$ and 0.002) in addition to those of Fig. 1. A further set of data, at $\chi=0.03$, have been omitted in the interests of clarity—their values lie between those of $\chi=0.004$ and $\chi=0.002$. By plotting the data against $2/N\chi$ we ensure that for any value of χ there is only one mean-field coexistence curve, which is displayed as a dotted-dashed line in the figure.

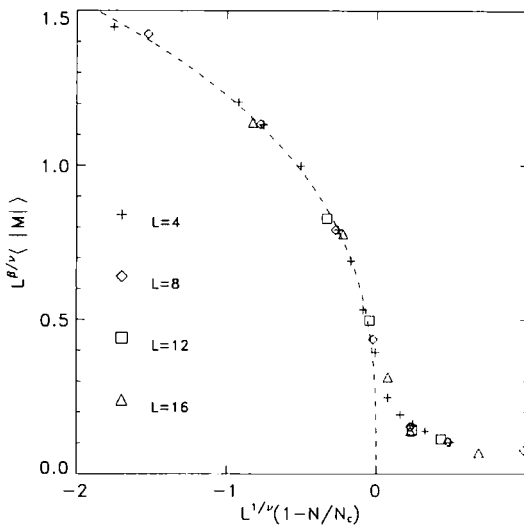


Fig. 4. Plot of the scaled order parameter in order to verify the finite-size scaling prediction, Eq. (6), in the case $\chi = 0.004$. The critical value is $N_c = 544$ and we have used the Ising values for the exponents $\beta = 0.324$, $\nu = 0.629$, with $v = \beta/\nu$ and $u = 1/\nu$. The dashed line denotes the limiting behavior $\langle |M| \rangle \propto |1 - N/N_c|^{v/u}$ for $L \rightarrow \infty$.

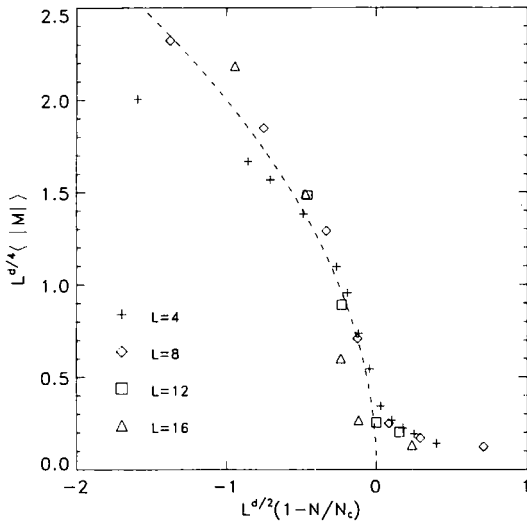


Fig. 5. Same as Fig. 4, but using instead the mean-field values for the exponents $u = 3/2$ and $v = 3/4$ and with $N_c = 542$.

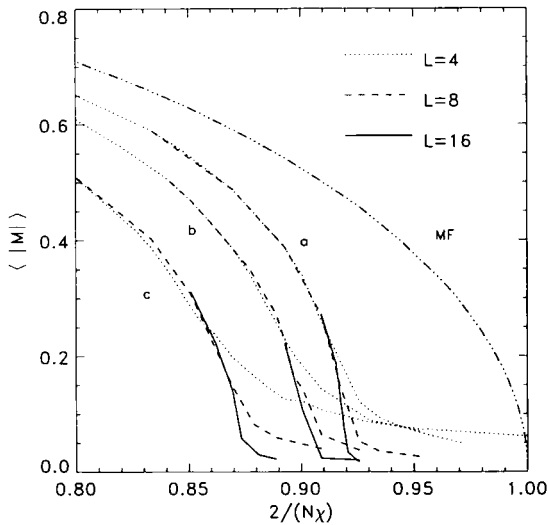


Fig. 6. The order parameter $\langle |M| \rangle$ as a function of polymer length N for different values of the Flory parameter χ : (a) $\chi = 0.004$; (b) $\chi = 0.002$; (c) $\chi = 0.001$. According to the mean-field theory (dot-dashed line, MF), the data should depend on N and χ only through the combination $2/(N\chi)$. It is clear that the deviation from mean-field behavior is quantitatively more pronounced for decreasing values of χ .

It can be seen from the figure that the discrepancy between (3) and the mean-field prediction *increases* with decreasing χ , or equivalently, with increasing values of N . This implies that the mean-field coexistence curve will not be recovered in the $N \rightarrow \infty$ limit of the model (3).

The only tendency away from Ising-like toward mean-field behavior that we observe on decreasing χ (increasing N) is that the distinction between an Ising-like and a mean-field description of the finite-size scaling behavior is not so clear-cut. For the case of $\chi = 0.001$, as with $\chi = 0.004$, we also examined the ratio $\langle M^2 \rangle / \langle |M| \rangle^2$ to establish bounds on N_c , obtaining $2285 < N_c < 2305$. The resultant scaling forms are indicated in Figs. 7 and 8 for $\chi = 0.001$ fixed. It is difficult to distinguish between the quality of the Ising-like scaling of Fig. 7 (with $N_c = 2300$) and the mean-field scaling of Fig. 8 (with $N_c = 2290$).

Although we have adopted the strategy of holding χ fixed and studying the behavior of (3) with varying polymer lengths, we could equally well have held N constant and considered varying χ . Physically, this should correspond to decreasing the temperature (assuming χ were purely temperature-dependent) for a given polymer length. As a final case, in Fig. 9 we fix $N = 2000$ and allow χ to vary. Once again, a clear discrepancy can be seen between the observed coexistence curve and that predicted by simple mean-field theory. From the ratio of $\langle M^2 \rangle / \langle |M| \rangle^2$ we estimate the

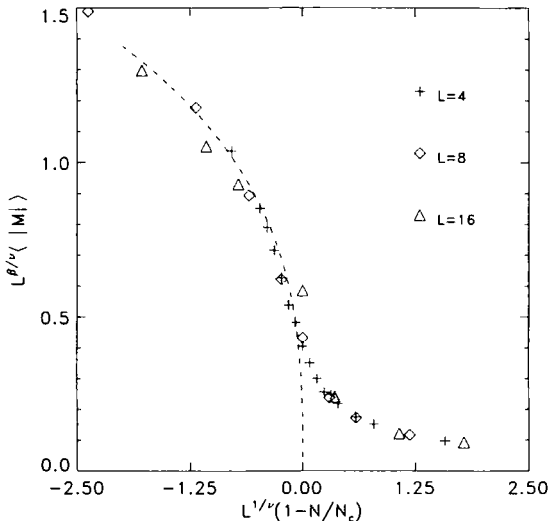


Fig. 7. Plot of the scaled order-parameter in order to verify the finite-size scaling prediction, Eq. (6), in the case $\chi = 0.001$. The critical value is $N_c = 2300$ and we have used the Ising values for the exponents $\beta = 0.324$, $\nu = 0.629$.

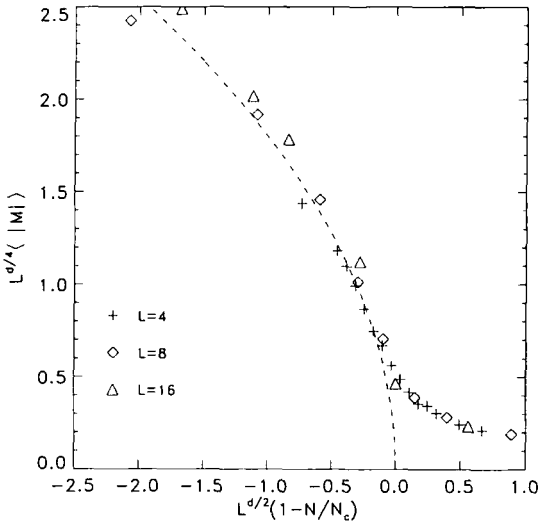


Fig. 8. Same as Fig. 7, but using instead the mean-field values for the exponents $\mu = 3/2$ and $\nu = 3/4$ and with $N_c = 2290$.

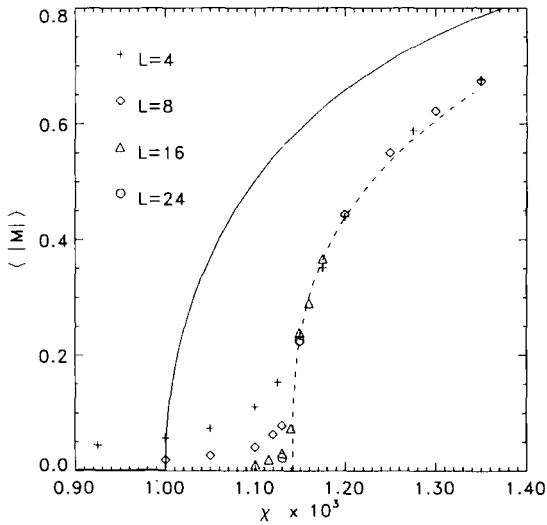


Fig. 9. The average order parameter $\langle |M| \rangle$ as a function of Flory interaction parameter χ with a fixed value $N = 2000$ of the polymer length for different system sizes L^3 . The solid line is the prediction of the mean-field theory. The dashed line is a fit to the behavior $\langle |M| \rangle \sim |1 - \chi/\chi_c|^\beta$ with $\chi_c = 0.001142$ and $\beta = 0.324$.

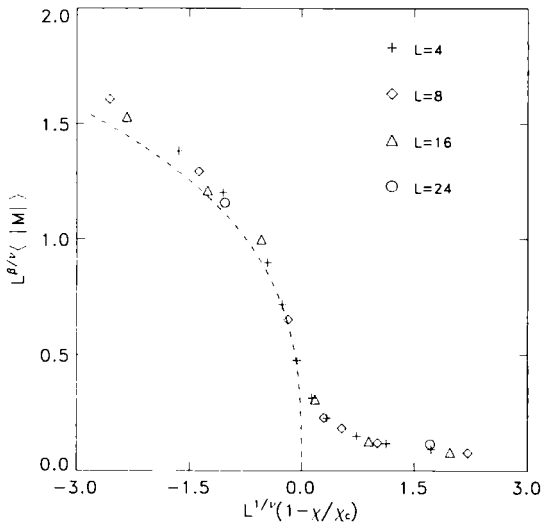


Fig. 10. Test of the finite-size scaling behavior as given by Eq. (7) with $N = 2000$. The Ising exponents $\beta = 0.324$, $\nu = 0.629$ are used. The critical value of the Flory-Huggins parameters is $\chi_c = 0.001142$. The limiting behavior $\langle |M| \rangle \propto |1 - \chi/\chi_c|^{t/\nu}$ for $L \rightarrow \infty$ is given by the dashed line.

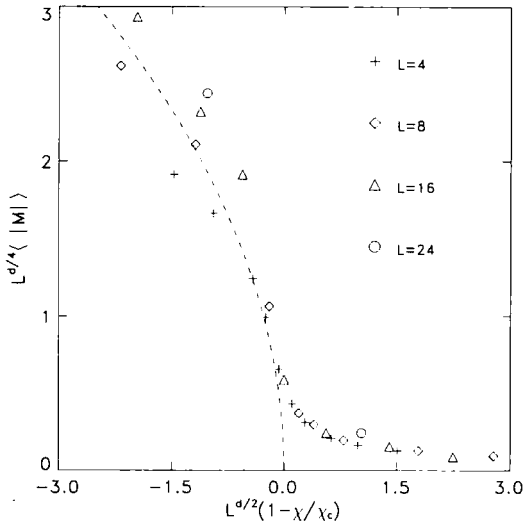


Fig. 11. As in Fig. 9, but using the mean-field exponents $u = 3/2$ and $v = 3/4$ and $\chi_c = 0.001140$.

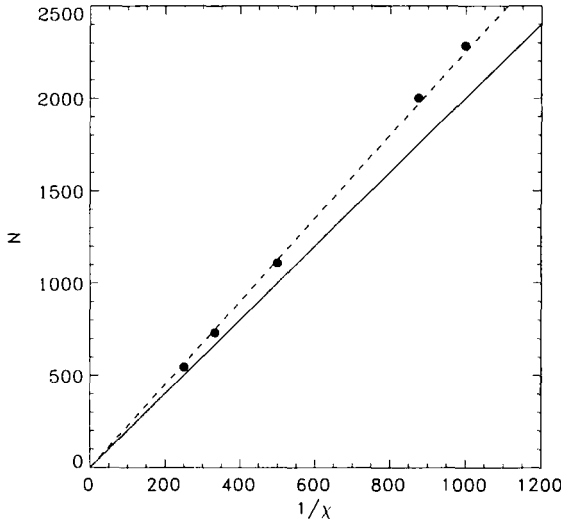


Fig. 12. Critical values of N and χ . The solid line is the mean-field prediction $\chi = 2/N$, the dashed line is a linear fit to the five data points, $\chi = 2.25/N$.

critical value of χ to be $1.13 \times 10^{-3} < \chi_c < 1.16 \times 10^{-3}$. The mean-field prediction, $\chi_c^{MF} = 2/N = 0.001$, thus underestimates χ_c by at least 13%. The finite-size scaling behavior is seen to be better for Ising-like scaling (Fig. 10, $\chi_c = 1.142 \times 10^{-3}$) than for mean-field scaling (Fig. 11, $\chi_c = 1.140 \times 10^{-3}$). In this case χ is the freely adjustable parameter controlling the weight of the single-site contribution in (3) relative to the interaction term, so we use

$$\langle |M| \rangle = L^{-v} f(L^u (1 - \chi/\chi_c)) \tag{7}$$

with, once again, $u = 1/v$, $v = \beta/v$ for Ising-like behavior and $u = d/2$, $v = d/4$ for mean-field scaling.

From the above five cases—four at fixed χ and one at fixed N —we have plotted the corresponding five critical points in Fig. 12. Also indicated is the mean-field theory prediction $N_c(\chi) = 2/\chi$, or equivalently, $\chi_c(N) = 2/N$. Although the observed relation between N and χ deviates from this behavior, it is nevertheless described well by a linear relation $\chi_c \propto N^{-1}$. We find $\chi_c \approx 2.25/N$.

4. DISCUSSION

The above analysis has revealed that the inclusion of the fluctuation term in (2) can have a considerable effect on the location of the coexistence

curve, although the actual weight of the term compared to the single-site contribution remains relatively small. The observed shift in the coexistence curve, including the model's prediction of the critical point [$N_c(\chi)$ for fixed χ , or $\chi_c(N)$ for fixed N] is an improvement over the naive mean-field solution of the Flory–Huggins lattice model in the sense that the correct tendency away from the mean-field result is displayed. The presence of the fluctuation term has the effect of enhancing the preference for of the one-phase solution, $\phi = \frac{1}{2}$, since the prefactor multiplying the square-gradient term in (2) displays a minimum at $\phi = \frac{1}{2}$. Thus, in effect, the entropic ($1/N$) term in $f_{\text{FH}}(\phi_x)$ encouraging the disordered one-phase behavior $\phi = \frac{1}{2}$ is strengthened, while the enthalpic (χ) term, which promotes the ordered two-phase behavior, $\phi = 0$ or 1 , is weakened. This has the result that the critical point $N_c(\chi)$ separating one-phase from two-phase behavior is increased (Fig. 6), or equivalently, $\chi_c(N)$ is increased (Fig. 9). It has already been observed^(4,6,23) that the critical temperature lies below that predicted by mean-field theory. This is consistent with our observations, as an increase in $\chi_c(N)$ at fixed N would imply a decrease in T_c , since $\chi \sim 1/T$.

While the discrepancy between the coexistence curve obtained from (2) and that given by mean-field theory is largest at the critical point of the model, the difference still remains significant reasonably far off criticality. For example, in Fig. 9, the curve is $\simeq 11\%$ away from the corresponding mean-field prediction at $\chi = 1.3 \times 10^{-3}$, i.e., at $1.14\chi_c$ ($= 1.3\chi_c^{\text{MF}}$). Interestingly, in a recent publication Holyst and Vilgis⁽⁹⁾ have found that, when fluctuation corrections are included in a self-consistent one-loop treatment, corrections to the naive mean-field prediction of the critical point can be as large as 10%, even for N up to $\sim 10^4$.

Despite the improvements brought about by (3) over the naive mean-field results, the desired tendency toward mean-field behavior as N increases is not fully recovered: while it is true that a finite-size scaling analysis cannot distinguish between the mean-field and the Ising values for the critical exponents at the largest values of N ($\simeq 2000$) considered here, the discrepancy between the coexistence curve given by (3) and that of mean-field theory in fact worsens as N is increased (see Fig. 6). This no doubt stems from the fact that, as N increases, and so χ must correspondingly decrease, the relative weight of the fluctuation term in (3) increases. While for $\chi = 0.004$ we observed that the weight of the square-gradient term was no more than a few percent, at $\chi = 0.001$ it had increased to just over 10%. This is possibly an indication that here we are encroaching upon the bounds of validity of the model; recall that the gradient term should remain small in magnitude relative to the single-site contribution f_{FH} . In this respect, the interaction term in (3), which has its source in the fluctuation term in (2), should really possess an N dependence or at least

an N -dependent interaction range, to recover the proper behavior in the $N \rightarrow \infty$ limit. The effective interaction range in a polymer solution does, after all, increase with N . As it stands, the model (2) only expresses an N dependence via its entropic contribution in f_{FH} .

One feature of the bare mean-field solution which does, however, seem to remain intact on including spatial fluctuations is the relation $\chi_c(N) \propto 1/N$. Only the proportionality constant is affected: instead of $\chi_c(N) = 2/N$, our data (Fig. 12) suggest $\chi_c(N) = 2.25/N$. Such a deviation from mean-field theory has also been observed in the bond-fluctuation model, where a linear relation between critical temperature and chain length was found to be maintained.⁽²²⁾

It may well be that, in order to observe the full crossover from Ising-like to mean-field scaling behavior, one would have to allow for a much larger variation in the corresponding crossover-scaling variable than we have attempted here. In the associated microscopic polymer model the pertinent crossover variable would be given by⁽³⁰⁾ $(1 - \chi/\chi_c)/G_i \propto (1 - \chi/\chi_c)N$, where $G_i \propto 1/N$ is the Ginzburg number. Thus one would have to vary N over several orders of magnitude to guarantee observing a complete crossover to mean-field critical behavior. Hence, while we certainly obtain Ising-like scaling behavior at our lowest values of N (≈ 500), our failure to observe unequivocal mean-field scaling at the largest values of N (≈ 2000) may be due to the fact that we cover only one decade in N . However, as mentioned above, this variation in N is apparently sufficient in order to at least manifest a trend away from Ising-like scaling toward mean-field scaling.

Admittedly, one should not place too much importance on the observation that the model (3) does not apparently display mean-field-like critical behavior, not even for large N —the model is, after all, only strictly valid when the concentration fluctuations are small. In the vicinity of the critical point this, of course, can no longer be true. Nonetheless, the model (3) *per se* does display critical behavior and, as seen above, this is best described by the Ising universality class rather than that of mean-field theory. In any case, even away from the critical region, where the model is valid, the discrepancy between the coexistence curve of the model and that of mean-field theory is still significant. As mentioned above, there is still an 11% discrepancy at $\chi = 1.14\chi_c$ ($= 1.3\chi_c^{MF}$) for $N = 2000$. This can have an important bearing on, for instance, off-critical quenches. Here this would correspond to a quench from the one-phase region into the two-phase region (i.e., from above to below the coexistence curve) at $\phi \neq \frac{1}{2}$. If one were not performing a “deep” quench (to well below the coexistence curve), then an accurate knowledge of the actual location of the coexistence curve becomes very important and it may prove dangerous to use the estimate given by naive mean-field theory for its location.

ACKNOWLEDGMENTS

Financial support from the DGICYT (Spain), grant number PB92-0046, is acknowledged. During this work B.M.F. was supported by a grant from the Ministerio de Educación y Ciencia (Spain).

REFERENCES

1. P. J. Flory, *Principles of Polymer Chemistry* (Cornell University Press, Ithaca, New York, 1986).
2. M. L. Huggins, *J. Chem. Phys.* **9**:440 (1941).
3. P. J. Flory, *J. Chem. Phys.* **9**:660 (1941).
4. A. Sariban and K. Binder, *J. Chem. Phys.* **86**:5859 (1987).
5. Th. G. Scholte, *J. Polymer Sci. A-2* **8**:841 (1970); C. T. Murray, J. W. Gilmer, and R. S. Stein, *Macromolecules* **18**:996 (1985); H. Ito, T. P. Russell, and G. D. Wignall, *Macromolecules* **20**:2213 (1987); F. S. Bates, *Macromolecules* **20**:2221 (1987).
6. A. Sariban and K. Binder, *Macromolecules* **21**:711 (1988).
7. E. A. Guggenheim, *Proc. R. Soc. A* **183**:203 (1944); T. A. Orofino and P. J. Flory, *J. Chem. Phys.* **26**:1067 (1957); M. L. Huggins, *J. Chem. Phys.* **75**:1255 (1971); M. Muthukumar, *J. Chem. Phys.* **85**:4722 (1986); M. G. Bawendi and K. F. Freed, *J. Chem. Phys.* **88**:2741 (1988).
8. K. S. Schweizer and J. G. Curro, *Phys. Rev. Lett.* **60**:809 (1988); *J. Chem. Phys.* **88**:7242 (1988); *Chem. Phys.* **149**:105 (1990).
9. R. Holyst and T. A. Vilgis, *J. Chem. Phys.* **99**:4835 (1993).
10. P. G. de Gennes, *J. Chem. Phys.* **72**:4756 (1980).
11. P. Pincus, *J. Chem. Phys.* **75**:1996 (1981).
12. K. Binder, *J. Chem. Phys.* **79**:6387 (1983).
13. D. W. Hair, E. K. Hobbie, A. I. Nakatani, and C. C. Han, *J. Chem. Phys.* **96**:9133 (1992).
14. G. Brown and A. Chakrabarti, *J. Chem. Phys.* **98**:2451 (1993).
15. J. D. Gunton, R. Toral, and A. Chakrabarti, *Physica Scripta* **T33**:12 (1990).
16. A. Chakrabarti, R. Toral, J. D. Gunton, and M. Muthukumar, *Phys. Rev. Lett.* **63**:2072 (1989); *J. Chem. Phys.* **92**:6899 (1990).
17. A. Sariban and K. Binder, *Polymer Commun.* **30**:205 (1989).
18. A. Sariban and K. Binder, *Macromolecules* **24**:578 (1991).
19. B. M. Forrest and D. W. Heermann, *J. Phys. (Paris) II* **1**:909 (1991).
20. K. Binder, *Phys. Rev. A* **29**:341 (1984).
21. H.-P. Deutsch and K. Binder, *Macromolecules* **25**:6214 (1993).
22. H.-P. Deutsch and K. Binder, *Europhys. Lett.* **17**:697 (1992).
23. H. P. Deutsch, *J. Chem. Phys.* **99**:4825 (1993).
24. S. Duane, A. D. Kennedy, B. J. Pendleton, and D. Roweth, *Phys. Lett. B* **195**:216 (1987).
25. B. Mehlig, D. W. Heermann, and B. M. Forrest, *Phys. Rev. B* **45**:679 (1992); *Mol. Phys.* **76**:1347 (1992); B. Mehlig and B. M. Forrest, *Z. Phys. B* **89**:89 (1992); A. L. Ferreira and R. Toral, *Phys. Rev. E* **47**:R3848 (1993).
26. K. Binder and D. W. Heermann, *Monte Carlo Simulations in Statistical Physics* (Springer-Verlag, Heidelberg, 1988).
27. H.-P. Deutsch, *J. Stat. Phys.* **67**:1039 (1992).
28. P. G. de Gennes, *Scaling Concepts in Polymer Physics* (Cornell University Press, Ithaca, New York, 1979).
29. G. S. Pawley, R. H. Swendsen, D. J. Wallace, and K. G. Wilson, *Phys. Rev. B* **29**:4030 (1984).
30. H.-P. Deutsch and K. Binder, *J. Phys. (Paris) II* **3**:1049 (1993).